STRESS MEASUREMENT DURING CRACK PROPAGATION IN METAL MATRIX COMPOSITES USING MICRO-RAMAN SPECTROSCOPY

AKM Asif Iqbal[1] and Yoshio Arai[2]

[1]Faculty of Manufacturing Engineering, University Malaysia Pahang, 26600, Pekan, Pahang Malaysia
Email: asifiqbal@ump.edu.my
[2]Division of Mechanical Engineering and Science, Saitama Universsity, 255, Shimo-Okubo, Sakura-ku, Saitama-shi, Saitama, Japan

Keywords: Cast Metal Matrix Composite (MMC), Crack propagation, Stress measurement, Raman spectroscopy

Abstract
The measurement of stress in the SiC particles during crack propagation was investigated by micro raman spectroscopy. The experiment was carried out *in situ* in the Raman spectroscopy. Experimental results showed that cracks due to monotonic loading propagated by the debonding of the particle/matrix interface and particle fracture. A high decrease in stress was observed with the interfacial debonding at the interface and with the particle fracture on the particle. Moreover, the critical tensile stresses for particle-matrix interface debonding and particle fracture developed in hybrid MMC were also estimated during the crack propagation.

1. Introduction

Aluminium based metal matrix composites (Al-MMCs) remain an interesting field of materials for technological development and have generated a significant amount of interest due to their high strength, stiffness, low density and higher operating temperatures compared to conventional engineering materials [1, 2]. Addition of ceramic reinforcement, such as SiC particles and Al_2O_3 whiskers, to conventional aluminum alloys, increases the modulus and fracture resistance of the Al-MMCs [2, 3]. Therefore, Al-MMCs are considered an attractive materials for many structural applications such as aerospace and automotive industries and wear applications, especially in the frictional area of braking system [2].

Although Al-MMCs have many advantages, their use in structural applications is sometimes hindered as their damage tolerance properties are relatively poor. These composites are often behaves like brittle material, especially when higher volume fractions of reinforcement is added to them [4]. Many studies have demonstrated the fracture behavior and the damage mechanism of ceramic particulate reinforced Al-MMCs. These studies concluded that the large differences in strain carrying capability of elastically deforming reinforcement and plastically deforming matrix alloy determine the key mechanism of fracture of Al-MMCs [5-7]. Owing to the constrained plastic flow of the matrix between the reinforcement particles in the MMCs, hydrostatic stresses develop in the matrix which plays an important role in the failure mechanism during monotonic and cyclic deformations [8]. Different constraint levels on the matrix flow control the local failure process (e.g. particle fracture, interfacial debonding and dimple fracture of matrix alloy). Among these, interfacial bonding between reinforcing particles and matrix alloy tends to be a dominating factor in local failure processes and the strengthening of Al-MMCs. Good interfacial bonding yields high dislocation density in the matrix

Excerpt from ISBN 978-3-00-053387-7

which increases the strength of MMCs, while low fracture toughness due to cracking of the reinforcing particles is given by good interfacial bonding [9]. Moreover, many researchers have investigated the fracture initiation mechanism of different types of MMCs and they have concluded that the damage often starts from the debonding of the interface of the reinforcement and matrix [9-11]. Besides, the authors of this article also investigated the fatigue fracture initiation and propagation mechanism in the cast hybrid MMC where they observed that the fracture was initiated by the debonding of particle and matrix located in the hybrid clustering region. The initiated microcracks then coalesced to other nearby microcracks in front of the crack tip and propagated through the particle/whisker-matrix interface [12]. Many researchers have investigated this phenomena numerically and found that stress concentration occurred on the particle-matrix interface and the area is highly vulnerable to fracture initiation [13,14]. In general, the crack propagation occurs in two ways. The first one is the partial debonding, i.e., the crack propagates along the reinforcement–matrix interface and no reinforcement breakage. The second one is the reinforcement fracture without debonding, i.e. the reinforcement fails as the load exceeds the reinforcements tensile strength [15]. Obviously, the above two phenomena could occur coincidentaly. It is supposed that if the interfacial crack spreads far enough, the bridging reinforcement will finally break after the reinforcement-matrix interfacial debonding. Therefore, it is important to identify and mesure the stress state of the reinforcing elements and the interface of the reinforcement-matrix during the crack propagation.

Micro-Raman spectroscopy (MRS) is a potential tool in the field of experimental mechanics with unique advantages, such as non-destructiveness, non-contact, high spatial resolution and depth focus. The stress or strain distribution on the reinforcement can be directly measured by MRS at microscale [16]. Several researchers have been used this tool to study the load transfer behavior of reinforcement debonding, bridging, pull-out and fracture [17, 18]. In the present study, micro raman spectroscopy is used to measure the stress that is developed in the SiC particles during crack propagation under monotonic loading in a cast hybrid MMC. The SiC particle-Al matrix interfacial fracture and the SiC particle fracture during monotonic loading are also observed in this study.

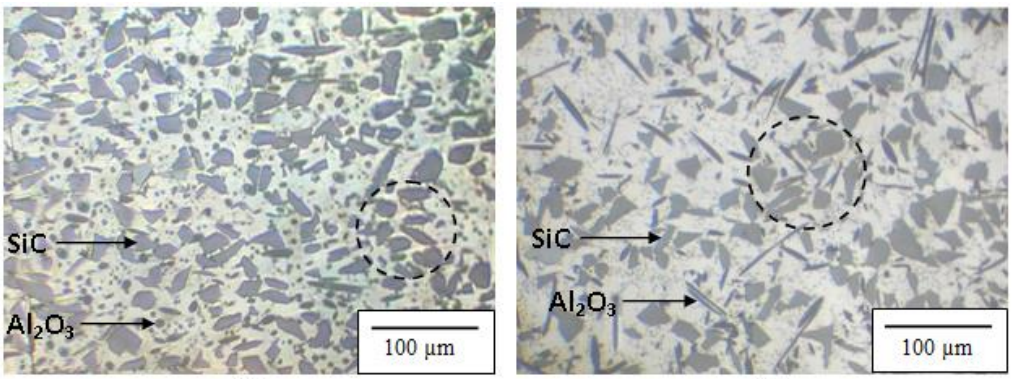

Figure 1. Microstructure in (a) lateral and (b) longitudinal cross sections of hybrid MMC

Table 1. Mechanical properties of reinforcement and tested materials

Parameters	Al_2O_3	SiC	Al alloy	Hybrid MMC
Young's modulus	380	450	70.0	142
Poisson's ratio	0.27	0.20	0.33	0.28
Yield strength (MPa)	-	-	131	166
Tensile strength (MPa)	-	-	262	228
Tensile elongation (%)			9.22	2.77

Excerpt from ISBN 978-3-00-053387-7

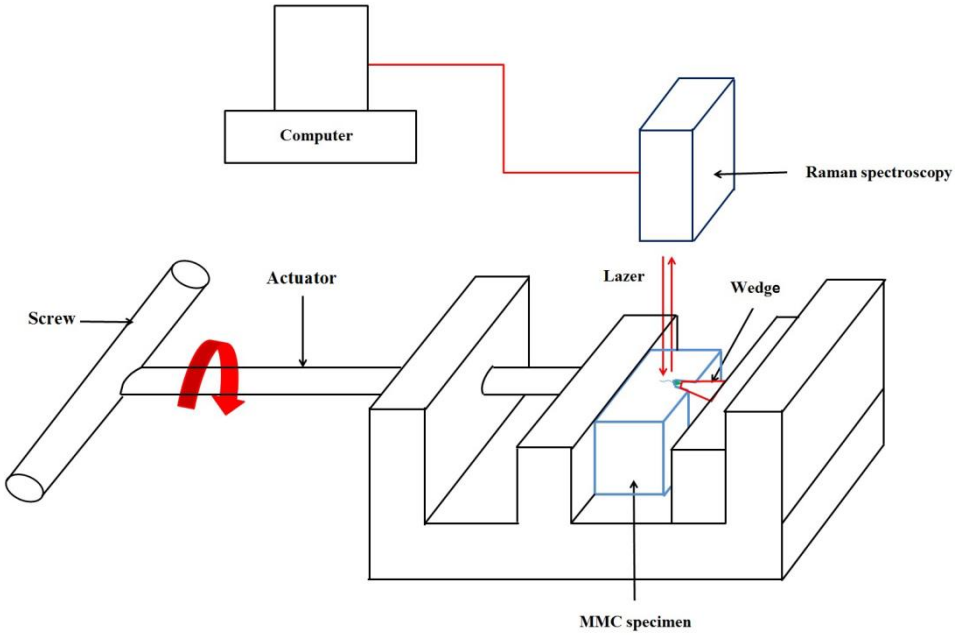

Figure 2. Schematic illustration of experimental setup

2. Materials and Experimental Procedures

Cast hybrid MMC material was used in this study to mesure the developed stress on the SiC particles. The hybrid MMC material was fabricated by the squeeze casting process swith 21 vol% SiC particles and 9 vol% Al_2O_3 whiskers as reinforcements and the aluminium alloy JIS-AC4CH as matrix. The casting pressure of 100 MPa was applied throughout the process adequate to overcome the resistance against flow and to press the melt into all the open pores of the hybrid preform. Finally, the material was heat treated using the T7 process. Figure 1 shows the microstructure of the hybrid MMC in lateral and longitudinal cross-sections. The SiC particles in the hybrid MMC were nearly rectangular shape with sharp corners and most of the Al_2O_3 whiskers were roller-shaped. The average length of SiC particles and the Al_2O_3 whiskers was 23 µm and 35 µm respectively. The average diameter of the Al_2O_3 whiskers was 2 µm. The Al_2O_3 whiskers were randomly oriented in the same plane as the longitudinal cross-section of the specimen. Clusters of SiC particles and Al_2O_3 whiskers were observed at frequent intervals in the hybrid MMC as indicated by the broken lines in Fig. 1a and 1b, respectively. The mechanical properties of reinforcement materials and hybrid MMC are shown in Table 1. The listed properties for the hybrid MMC are along the longitudinal direction. A rectangular notched specimen is used for the experiment with the length of 10 mm, thickness of 8 mm and width of 8 mm. The machined surfaces of the specimens were polished by using a polishing machine with 15, 3, and 1 µm diamond particles sequentially until all scratches and surface machining marks were removed and became smooth enough to prevent attenuation of the scattered light from the specimen. The experiment was carried out *in situ* in the Raman spectroscopy with special loading fixture consists with a wedge and a mechanical actuator. A schematic illustration of the experimental setup is shown in Figure 2**.** By rotating the screw in the fixture, the wedge moves towards the notch which provide crack face opening of the specimen. The wedge angle is 5.4 deg. The rotation of the screw is manually controlled and monitored carefully. The data presents in this article are in relation with the rotation of the screw in the fixture. Strain gauge was attached at the bottom of the specimen to determine the contact of the wedge to the specimen notch. The strain data was recorded by a computer data acquisition system. All tests were carried out at room temperature. The initiation and propagation of micro-cracks were observed by the optical microscope attached in the micro-Raman spectroscopy.

The Raman microscopic studies were carried out on a laser micro-Raman spectrometer (Lamda vision LV-RAM 532). A green laser with a wavelength of 532 nm and a power of 70 mW was used. The

Excerpt from ISBN 978-3-00-053387-7

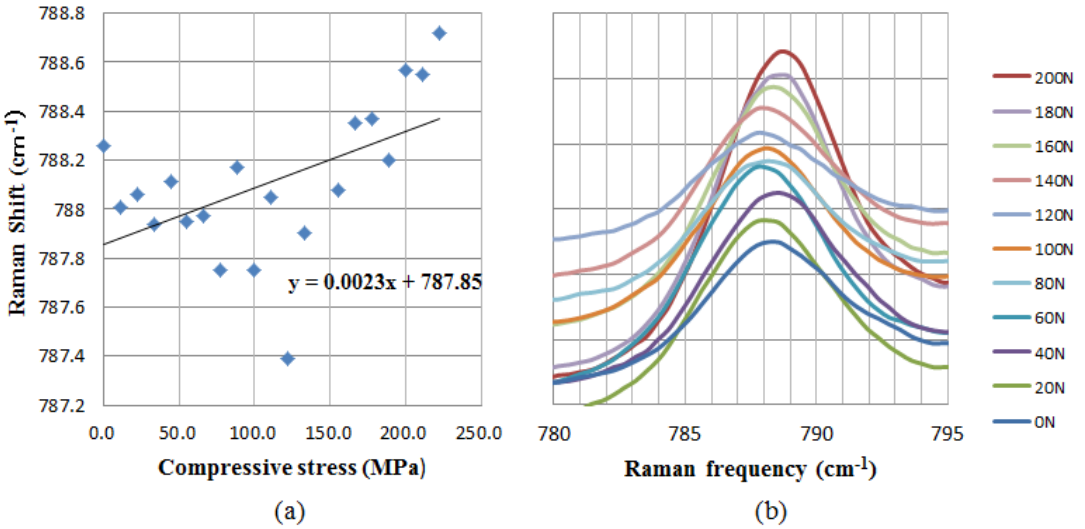

Figure 3. (a) Raman gage factor of SiC particle, (b) Raman spectrum in different loads.

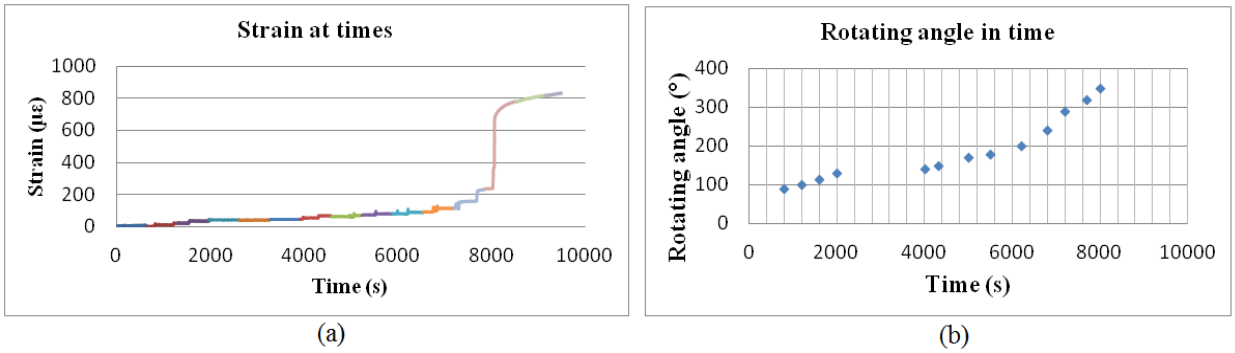

Figure 4. (a) Change of strain in different times, (b) Rotation of screw in different times.

laser beam was focused to a 2 µm diameter spot on the specimen surface using an optical microscope with X50 objective lens. The backscattered light was dispersed by leading it to the spectrometer through the microscope objective. Raman spectra were recorded using a charge coupled device (CCD). The Raman frequencies of the Raman bands were obtained with an accuracy of ±0.3cm^{-1}.

3. Results and Discussion

To analyze the stress concentration and crack propagation in the cast hybrid MMC by Raman spectroscopy, first, the Raman gage factor of SiC particle needs to be determined. Therefore, a SiC monolithic bar with the length of 8.3 mm, width of 1 mm and height of 0.9 mm is selected. An axial compressive load of 200 N was applied to the SiC bar and Raman peaks were observed. Figure 3 shows the results of Raman gage factor and the Raman spectrum of SiC bar in different load condition. It is evident from Fig. 3 that the peak frequency has the tendency of increasing upward (Fig. 3a) with increasing load, indicating the development of compressive stress in SiC bar. The peak of Raman shift was found to be 788 cm^{-1} and the gage factor (GF) was calculated to be 0.0023 cm^{-1} /MPa (as indicated in Fig. 3a).

Figure 4 shows the results of change in strain in different times and different angles of the rotating screw throughout this experiment. Figure 4(a) indicates the crack initiation at the notch during the application of monotonic load applied by the movement of actuator of the fixture as a sudden increase of the strain. From 0 to 7000s, the screw was rotated to 300º (Fig. 4b), but no significant change in strain was observed. This means the wedge did not contact the surface of the notch at this stage. At

Excerpt from ISBN 978-3-00-053387-7

7700s and 320º rotation of the screw, the strain started increasing, indicating the first contact of the wedge to the notch. However, the rapid increment of the strain was observed in 350º rotation of the screw at 8000s, indicating the crack initiation at the tip of the notch at this stage. This result clearly demonstrated that the crack initiated at 30º increment in rotation of the screw from the absolute value of rotation angle 320º at which the wedge contacted the notch. In the following discussion we use the increment value in rotation from the 320º and just call it 'rotation angle'. The wedge loading always gives a critical stress field ahead of a main crack tip which arrests at a critical length. So, the rotation angle implies the advance in loading process just qualitatively.

The propagation of the crack on the surface of the hybrid MMC material can be followed from the optical micrograph observation in Raman spectroscopy. The optical micrographs of the crack propagation obtained on the surface at different rotating angles of the screw are shown in Figure 5. Several SiC particles have been chosen and numbered to observe and analyze the relation between the stress in SiC particles and propagation of the interface crack. At 30º rotation of the screw (Fig. 5a), the crack initiated at the tip of the notch. At 35º rotation of the screw, the main crack tip reached the particle 8 and its length from the notch was increased to 0.95 mm (Fig. 5b). Few secondary cracks were observed initiated in front of the main crack tip as well as parallel to the main crack. At 40º rotation of the screw, the secondary cracks joined with the main crack and the crack length further extended to 1.16 mm (Fig. 5c). The interface debonding between SiC particle 8 and Al alloy matrix was seen at this stage of crack propagation. The crack moved further as the rotation of the screw continued and at 45º rotation of the screw, several SiC particles were found debonded from matrix and both the particles 8 and 14 were found fractured at this stage (Fig 5d). Further loading resulted in the unstable fracture of the specimen. Figure 6 indicates the optical micrograph of the particle 8 in different rotating angle and the behavior of propagating crack at the interface between particle 8 and matrix alloy. The number 8 written on the figures indicating the particle number 8 and red spots on the particle indicate the Raman laser spots. At the initial stage, no cracks were observed at the interface of the particle (Fig. 6a). Besides, at 35º rotation of the screw, the main crack propagated along the interface of the particle 8. At the same time, another crack was observed in front of the main crack tip. The presence of arrested crack at this stage indicated the interface debonding seems to be stable.

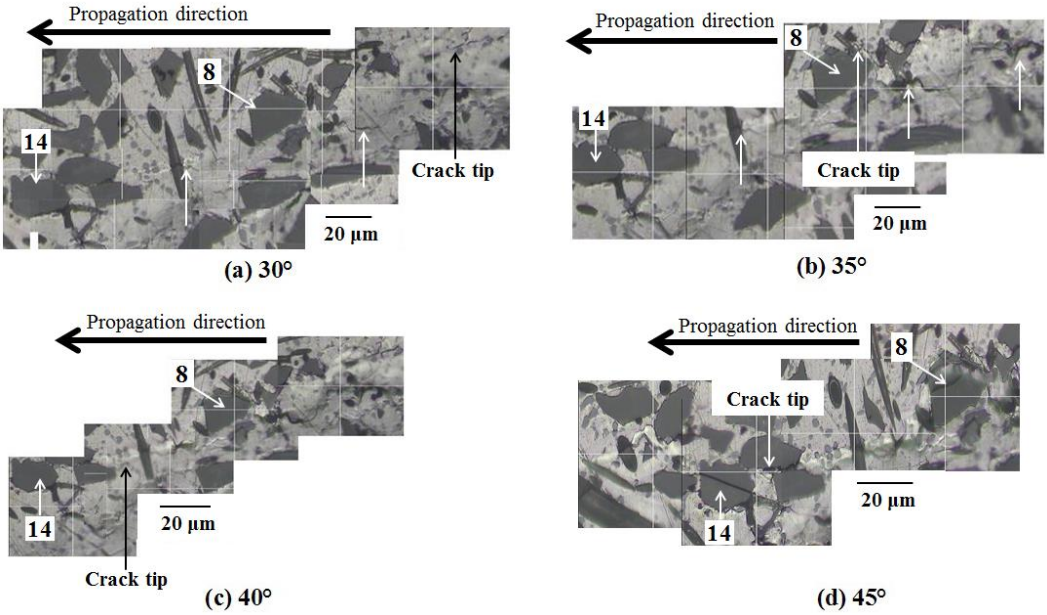

Figure 5. Crack propagation in hybrid MMC at different rotating angles of the screw

Excerpt from ISBN 978-3-00-053387-7

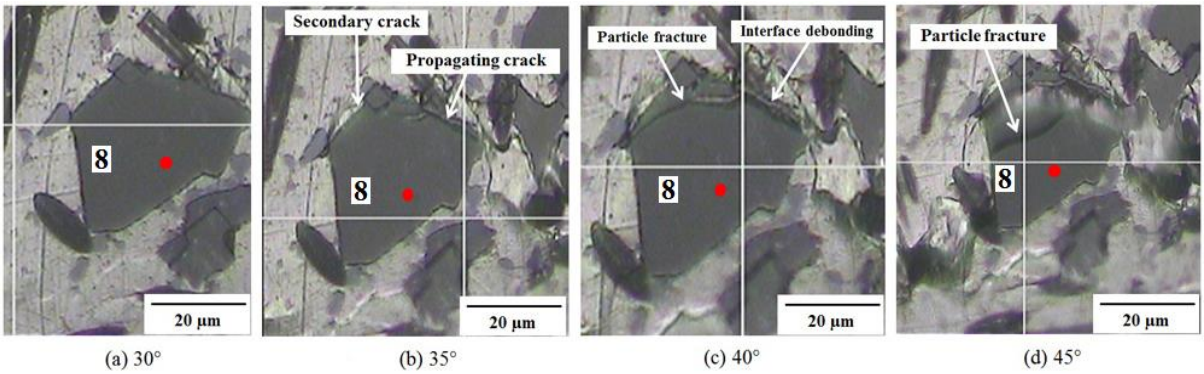

Figure 6. Interface crack on particle 6 at different rotating angle of the screw.

The crack then further propagated by deflecting into SiC particle at 40º rotation of the screw (Fig. 6c). However, the middle part of this particle was found fractured at the higher rotating angle of the screw (Fig. 6d). The same phenomena were also observed in particle 14. The results of the Raman spectrum taken on the particle 8 in different rotating angle is shown in Fig 7. It can be seen that the Raman peak was increased to 785.51 cm^{-1} at the angle of 35º when the interfacial debonding occured at particle 8. The Raman peak also increased when the crack deflected into the particle at 40º rotation. Moreover, at 45º rotating angle, the Raman peak was observed 786.38 cm^{-1}. At this stage particle 8 became fractured as shown in Fig 6d. From the obtained peak wave number, the change in stress for debonding to take place in particle 8 is calculated by using the SiC gage factor and the result is presented in Table 2. The change in stress measured in the particle 8 after debonding from the matrix was calculated to be -483 MPa (- sign indicates a decrease in stress). The decrease in stress compared to the un-cracked state means an unloading of originally tensile stress developed due to the opening of crack under wedge loading. The change in stress due to crack deflection from the interface to the SiC particle was -161 MPa. Besides, the maximum change in stress measured in the particle 8 after particle fracture was found to be -217 MPa at the angle of 45º of the screw. The accumulated change in stress from the un-cracked state to the particle fracture was -861 MPa which means 861 MPa was the estimated value of tensile stress developed in the particle located just ahead of the crack tip before fracture. The similar high value of change in stress was also measured in particle 14.

From the above results, it is obvious that the crack due to the weged-type monotonic load propagated along the particle-matrix interface as well as through the particle in the hybrid MMC. The local effective stress, which is acting on the particle ahead of the crack tip reaches extreamly high values (800 – 900 MPa). While the high values of stress have been reported in the simulation work [10], this study presented them through micro-Raman spectroscopy *in situ* fracture experiment. At the fracture stress under monotonic loading condition, the reinforcing particles deformed elastically within the plastically deforming matrix alloy. Thus, a large strain mismatch occurs between these two materials. For this mismatch of strain, a consequent concentration of stress is generated in the particles and at the interface between the reinforcing particles and matrix alloy. These stresses cause the interface separation of particle- matrix as well as the particle fracture, and the crack propagates till the final failure occur.

3. Conclusions

The crack propagation and the fracture mechanism, especially the change in stress state of the reinforcing particles in hybrid MMC during crack propagation is investigated by micro Raman spectroscopy. The following conclusions were made:
(1) Cracks propagated by the debonding of the particle/matrix interface and particle fracture. Few secondary cracks were generated in front of the main crack tip, which were coalesced with the main crack and final failure occurred.

Excerpt from ISBN 978-3-00-053387-7

(2) The Raman spectroscopy confirmed that a high decrease in stress (several hundreds in MPa) occurred with the interfacial debonding at the interface and with the particle fracture on the particle. Therefore, the critical tensile stresses for particle-matrix interface debonding and particle fracture developed in hybrid MMC were estimated during the propagation of the crack in monotonic loading.

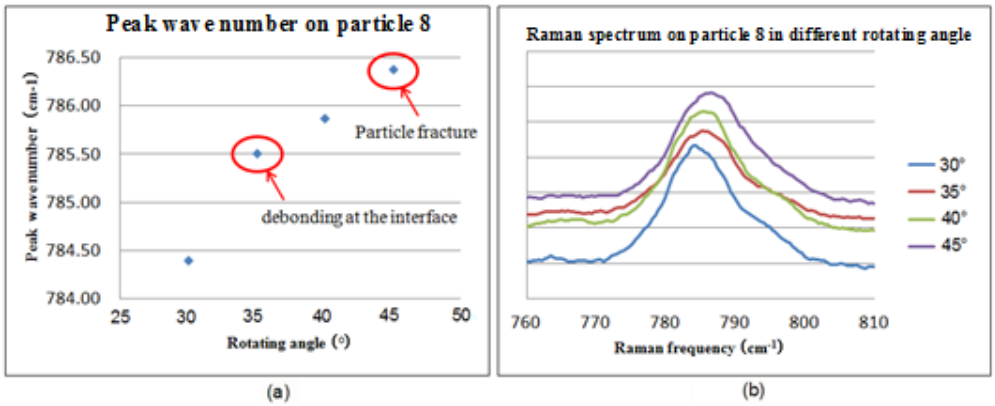

Figure 7. Raman spectroscopy on particle 8 in different rotating angle (a) peak wave number (b) Raman spectrum

Table 2: Change of accumulated stress on particle 8 in different rotating angle.

Rotating angle (°)	Peak wave number (cm^{-1})	Change in stress (MPa)	Accumulated change in stress (MPa)
30	784.4		
		-483	
35	785.51		-483
		-161	
40	785.88		-643
		-217	
45	786.38		-861

References

[1] T.W. Clyne, and P. J. Withers. An introduction to metal matrix composites. *Cambridge University Press*, Cambridge; 1993.

[2] S. Suresh, A. Mortensen and A. Needleman. Fundamentals of Metal Matrix Composites. *Butterworh/Heinemann*, London, 1993.

[3] J.E. Allison, L.C. Davis, and J.W. Jones. Composites Engineering Handbook, ed. P. K. Mallick, *Marcel Dekker,New York*. p. 941, 1997.

[4] A. Miserez, A. Rossoll, and A. Mortensen. Investigation of crack-tip plasticity in high volume fraction ceramic particle reinforced metal matrix composites. *Engineering Fracture Mechanics*, 71:2385–406, 2004.

[5] A.L. Chen, Y. Arai and E. Tsuchida. An experimental study on effect of thermal cycling on monotonic and cyclic response of cast aluminium alloy-SiC particulate composites. *Composites B*, 36:319–30, 2005.

Excerpt from ISBN 978-3-00-053387-7

[6] T.S. Srivatsan and M. Al-Hajiri. The fatigue and final fracture behavior of SiC particle reinforced 7034 aluminum matrix composites. *Composites B*, 33:391–404, 2002.

[7] X.Q. Xu and D.F. Watt. A finite element analysis of plastic relaxation and plastic accumulation at second phase particles. *Acta Materialia*, 44,801–11, 1996.

[8] J. Llorca, S. Suresh and A. Needleman. An experimental and numerical study of cyclic deformation in metal matrix composites. *Metallurgical Transactions A*, 23, 919–934, 1992.

[9] E.Y. Chen, L. Lawson and M. Meshii. The effect of fatigue microcracks on rapid catastrophic failure in Al–SiC composites. *Materials Science and Engineering* A, 200:192–206, 1995.

[10] A. Mkaddem and M. Mansori. On fatigue crack growth mechanisms of MMC: reflection on analysis of multi surface initiations. *Materials and Design*, 30:3518–3524, 2009.

[11] Z.Z. Chen and K. Tokaji. Effects of particle size on fatigue crack initiation and small crack growth in SiC-particulate reinforced aluminium matrix composites. *Materials Letters*, 58:2314–2321, 2004.

[12] A.A. Iqbal, Y. Arai and W. Araki. Effect of hybrid reinforcement on crack initiation and early propagation mechanisms in cast metal matrix composites during low cycle fatigue. *Materials and Design*, 45:241-252, 2013.

[13] Y.W. Yan, L. Geng and A.B. Li. Experimental and numerical studies of the effect of particle size on the deformation behavior of the metal matrix composites. *Materials Science and Engineering A*, 448:315-325, 2007.

[14] A.A. Iqbal, Y Arai, W. Araki. Effect of reinforcement clustering on crack initiation mechanism in a cast hybrid metal matrix composite during low cycle fatigue. *Open journal of composite materials*, 3:97-106, 2013.

[15] J.A. Bennett and R.J. Young. A strength based criterion for the prediction of stable fibre crack-bridging. *Composite Science and Technology*, 68:1282–1296, 2008.

[16] L. Zhenkun, W. Quan and Q. Wei. Micromechanics of fiber–crack interaction studied by micro-Raman spectroscopy:Broken fiber. *Optics and lasers in engineering*, 51:1085-1091, 2013.

[17] Z.K Lei, Q. Wang, Y.L. Kang, G. Liu and H. Yun. Stress transfer of single fiber/micro droplet tensile test studied by micro-Raman spectroscopy. *Composites A*, 39:113–8, 2008.

[18] Z.K Lei, Q. Wang, Y.L. Kang, X.M. Pan. Stress transfer in microdroplet tensile test:PVC coated and uncoated Kevlar-29 single fiber. *Optics and lasers in engineering*, 48:1089–95, 2010.

Excerpt from ISBN 978-3-00-053387-7